

Augmenting the sensing performance of entangled photon pairs through asymmetry

Yoad Michael, Isaac Jonas, Leon Bello, Mallachi-Ellia Meller, Eliahu Cohen, Michael Rosenbluh, and Avi Pe'er
Bar-Ilan University, 5290002 Ramat-Gan, Israel
(Dated: February 28, 2022)

We analyze theoretically and experimentally cases of asymmetric detection, stimulation and loss within a quantum nonlinear interferometer of entangled pairs. We show that the visibility of the $SU(1,1)$ interference directly discerns between loss on the measured mode (signal), as opposed to the conjugated mode (idler). This asymmetry also affects the phase sensitivity of the interferometer, where coherent seeding is shown to mitigate losses that are suffered by the conjugated mode, therefore increasing the maximum threshold of loss that still allows for sub-shot-noise phase detection. Our findings can improve the performance of setups that rely on direct detection of entangled pairs, such as quantum interferometry and imaging with undetected photons.

The main goal in quantum interferometry is to measure small phase shifts with very high sensitivity, beyond what could normally be achieved with classical light schemes that are limited by shot-noise [1, 2]. The major resource for sub-shot-noise interferometry is squeezed light [3–9], which is simple to generate by parametric down conversion and is widely utilized, e.g. by LIGO and VIRGO [10–16]. The most common interferometric configuration is the Mach-Zehnder or Michelson interferometer, where the input beam is split to two paths by a beam-splitter (BS) and then recombined, with one beam experiencing a relative phase shift. The drawback of this scheme is the mixing of the optical state with vacuum fluctuations through the unused port of the first BS [17], which limits the phase sensitivity to the shot-noise limit, and can be mitigated by injecting the unused port with squeezed vacuum [18].

An alternative and very useful interferometric approach is to replace the two beam-splitters with optical parametric amplifiers (OPAs) [19]. An OPA produces entangled photon pairs (or squeezed light), each comprised of two correlated spectral modes known as the signal and idler, that have a well-defined phase relation with respect to the pumping field. The OPA can be thought of as a two-mode squeezer that amplifies one quadrature of the combined signal-idler field, and attenuates the other quadrature [20, 21]. Placing two consecutive OPAs with a phase shift in-between yields a phase-dependent output (See Fig. 1a), similarly to the interference output of a beam-splitter, with one key advantage over its classical counterpart: if no loss exists between the two OPAs, the optical state is not mixed with external vacuum, yielding sub shot-noise phase sensitivity with no need for external squeezing [22, 23]. This configuration is known as the $SU(1,1)$ interferometer [24–26].

In addition to the improved sensitivity, the $SU(1,1)$ interferometer is a highly flexible scheme that was previously utilized in various forms: A balanced configuration where the intensity is measured directly [27] or through parity detection [28], a truncated configuration [29, 30] where the second OPA is replaced by standard homodyne detection, a non-balanced configuration where the second

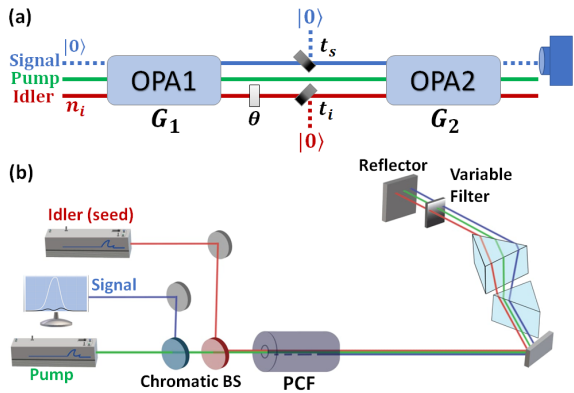


FIG. 1. Conceptual and experimental overview of the system. (a) Nonlinear $SU(1,1)$ interferometer with losses. Signal and idler pairs are amplified by OPA1, with the pump providing the parametric gain. A relative phase shift θ is applied, and the modes experience independent photon losses (which mixes the quantum state with vacuum), represented by transmission coefficients $t_{s,i}$. The mixed state is amplified by OPA2, where nonlinear interference occurs. (b) Experimental realization using a photonic crystal fiber (PCF) as both OPAs. A 786nm pump laser is coupled into the PCF, where signal and idler pairs are generated through four-wave mixing. The beams are separated chromatically using a prism-pair and the transmission of the signal and idler can be controlled independently using variable transmission filters. All beams are retro-reflected back into the PCF for a second pass, where the nonlinear interference occurs. The signal is filtered from the pump and idler using a chromatic beam splitter and then measured with a spectrometer. For the stimulation, the PCF is seeded with an 878nm CW laser at the idler.

OPA is set to a higher gain for broadband parametric homodyne measurement [31, 32] and overcoming detection loss [33–35], etc. In addition to direct phase sensing, the improved signal-to-noise due to the squeezing was also harnessed for various other applications, such as Raman spectroscopy [36, 37] and atomic force microscopy [38]. The $SU(1,1)$ interferometer can operate in multiple regimes, depending on the intensity of the fields: quantum or classical [39], spontaneous or stimulated [40, 41], with optical losses shown to degrade the squeezing [42–44].

While the SU(1,1) interferometer is typically discussed in the context of squeezing-enhanced detection, a different property of the entanglement between the signal and idler was utilized for quantum imaging with undetected photons [45]: The IR spectra of a molecular sample that absorbs light at the idler wavelengths, was inferred from the visibility of nonlinear interference measured at the signal wavelength [46–48], which is far more optically-accessible. In this type of schemes, the symmetry between the two modes that comprise the pair is inherently broken: while the idler experiences photon loss, it is the signal that is measured. This effect of asymmetry between the modes is critical both for quantum imaging and squeezing-enhanced applications, yet is usually not elaborated upon and is given as part of the framework of the experimental setup.

Here we explore theoretically and experimentally the effect of asymmetric optical loss, asymmetric measurement and asymmetric seeding on the SU(1,1) interference of entangled photon pairs. We show that the quantum interference is critically affected by whether the mode (signal or idler) that experiences loss, is also the one that is measured, or the conjugate one. When measuring the interference at the signal mode, we show that the visibility of interference can be twice as high when losses are applied on the signal compared to the idler. The phase-sensing performance of the interferometer is also affected: In the spontaneous regime, higher phase sensitivity is observed when losses are applied on the measured mode (signal) than on the conjugated mode (idler). When the conjugated mode is coherently seeded, it withstands higher degree of loss while maintaining sub shot-noise phase sensitivity.

We start with the mathematical description of the OPA. An OPA is a nonlinear gain medium that generates entangled signal and idler pairs from a strong pump [49–51]. The quantum state of the entangled pairs is described by the input-output relations of the field operators before and after passing the OPA $\hat{a}_{s,i}^{(out)} = \cosh(G)\hat{a}_{s,i}^{(in)} + \sinh(G)\hat{a}_{i,s}^{\dagger (in)}$, where $\hat{a}_{s,i}^{(in,out)}$ are the field operators of the signal/idler at the input and output of the OPA, and G is the parametric gain. We place two OPAs with gains $G_{1,2}$ one after the other, with a phase shift θ and optical loss applied between them (See Fig. 1a).

The most general expression for the photon number at the signal output of the interferometer is (see the Supplemental Material for details):

$$\begin{aligned} \langle \hat{N}_s \rangle = & \frac{1}{2}(n_i + 1) \sinh(2G_1) \sinh(2G_2) \cos(\theta) t_i t_s \\ & + (n_i + 1) \sinh^2(G_2) \cosh^2(G_1) t_i^2 \\ & + (n_i + 1) \sinh^2(G_1) \cosh^2(G_2) t_s^2 \\ & + \sinh^2(G_2) (1 - t_i^2), \end{aligned} \quad (1)$$

with a vacuum input at the signal port and a co-

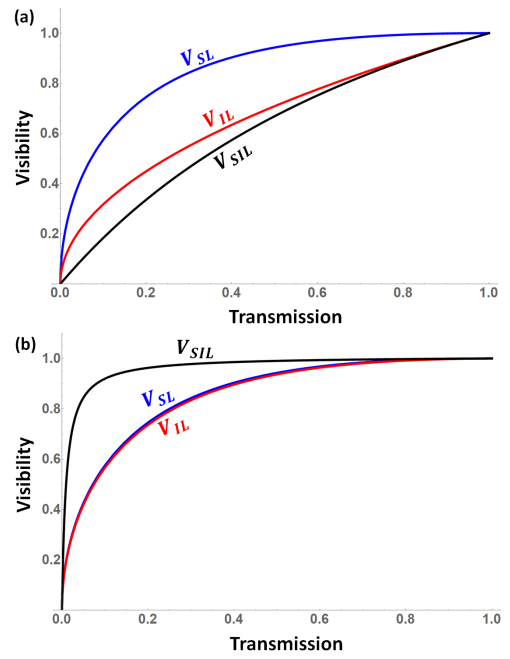


FIG. 2. The theoretical visibility of nonlinear interference as a function of the transmission ($t_{s,i}^2$) of the signal (V_{SL} , blue), idler (V_{IL} , red) and equal transmission (V_{SIL} , black), for (a) the spontaneous $n_i = 0$ and (b) idler-stimulated $n_i = 50$ cases, at the low gain regime of $G_1 = G_2 = 0.1$. The interference is measured at the signal mode. For the spontaneous case, the highest visibility is observed when losses are applied on the measured mode (V_{SL}), highlighting the asymmetry to loss between the measured and conjugated modes. For the stimulated case, the loss asymmetry between the two modes breaks ($V_{SL} = V_{IL}$), with equal loss (V_{SIL}) achieving the highest visibility, in correspondence to Eqs. 2-4.

herent state of n_i average photons at the idler port, and where $t_{s,i}$ is the transmission of the signal and idler. To understand the physical meaning of the different terms in this general expression, let us first consider a simplified case with no losses $t_s = t_i = 1$, and phase of $\theta = 0, \pi$ (corresponding to constructive and destructive interference). The expression then reduces to $\langle \hat{N}_s \rangle = (n_i + 1) \sinh^2(G_1 \pm G_2)$, with the seed photons n_i acting as a classical stimulation for the pair generation. When losses are introduced, the interference terms (first three terms of Eq.1) are transmitted, but a non-interfering term of $(1 - t_i^2) \sinh^2(G_2)$ is introduced from the spontaneous amplification of the quantum vacuum by OPA2. Note that this term arises from loss on the conjugated mode - hinting at the asymmetry to loss.

To understand the consequences of this term, we proceed to define the visibility (contrast) of interference as $V = \frac{\langle \hat{N}_s \rangle_{\theta=0} - \langle \hat{N}_s \rangle_{\theta=\pi}}{\langle \hat{N}_s \rangle_{\theta=0} + \langle \hat{N}_s \rangle_{\theta=\pi}}$, where $V = 1$ indicates maximum distinction between constructive and destructive interference. For the SU(1,1) interferometer we present here, the three interesting cases are the visibility due to losses on

the signal (V_{SL}), on the idler (V_{IL}), or on both (V_{SIL}), which can all be derived from Eq. 1.

Let us start with the simple case of a balanced amplifiers (no pump losses) $G_1 = G_2 = G$, and derive the expressions of the visibility as a function of the transmission (plotted in Fig. 2). When loss is applied only on the signal ($t_i = 1$) the visibility is

$$V_{SL} = \frac{2t_s}{t_s^2 + 1}, \quad (2)$$

which is independent of the gain and stimulation, and approaches 100% for $t_s \rightarrow 1$, as shown by the blue curve in Figs. 2a and 2b. Next, for losses only on the idler ($t_s = 1$), the visibility is

$$V_{IL} = \frac{2(n_i + 1)t_i \cosh^2(G)}{(n_i + 1)(t_i^2 + 1) \cosh^2(G) + 1 - t_i^2}. \quad (3)$$

Generally $V_{IL} < V_{SL}$ (shown by the red curve in Fig. 2) indicating that higher visibility is observed when applying loss on the measured mode (signal) than on the conjugated mode (idler), with $V_{IL} \rightarrow \frac{2t_i}{t_i^2 + 1}$ for high values of G and n_i (Fig. 2b). Intuitively, since the signal and idler undergo nonlinear interference together, one might expect $V_{SL} = V_{IL}$, yet the question of which of the modes is measured (in our case, the signal) breaks the symmetry between the entangled pairs and distinguishes V_{SL} from V_{IL} .

The last interesting case is equal (symmetric) loss on both the signal and idler ($t_s = t_i = t$):

$$V_{SIL} = \frac{2(n_i + 1)t^2 \cosh^2(G)}{2(n_i + 1)t^2 \cosh^2(G) + 1 - t^2}, \quad (4)$$

Which for the spontaneous case has the lowest visibility (black curve in Fig. 2a), yet approaches 100% for large values of G and n_i , even for low values of t (Fig. 2b).

Since the pump of the OPAs is assumed completely classical, we do not consider loss on the pump field in a quantum manner. Introducing loss on the pump between the two OPAs simply lowers the nonlinear gain of OPA2 $G_2 = t_p^2 G_1$ where t_p is the transmission of the pump. This gain imbalance can always be either compensated experimentally or calibrated and accounted for in the analysis, as we do in our experimental measurements.

Although the visibility can be improved by higher parametric gain, the gain of the first OPA G_1 - unfortunately cannot be enhanced indefinitely due to adverse non-linear effects (attributed to high pump powers) that degrade the squeezing [52]. On the other hand, stimulating the interferometer with a coherent seed increases the visibility and can be arbitrarily strong. Thus, throughout this work we will focus on the lower gain regime and a strong coherent seed.

In our experiment, we constructed a 4WM-based SU(1,1) interferometer, as shown in Fig. 1b. Our pump

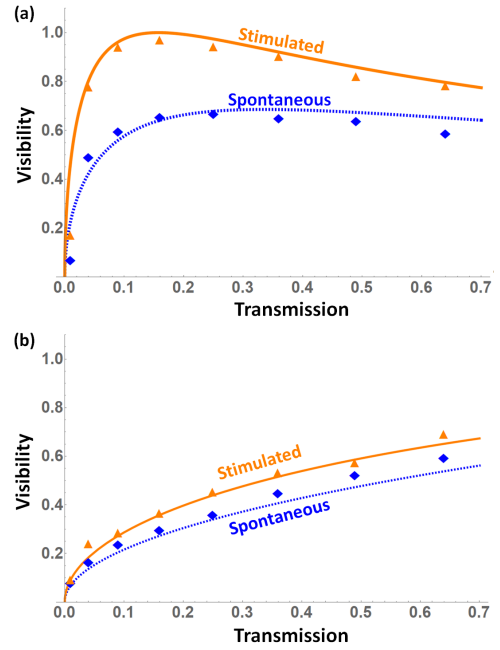


FIG. 3. Experimental and theoretical visibility as function of the transmission ($t_{s,i}^2$) of the signal (a) and idler (b), for the spontaneous ($n_i = 0$, blue, dashed) and strongly stimulated cases ($n_i = 10000$, orange, solid), with $G_1 = 0.45$, $G_2 = 0.2$. The initial loss of the signal was lower than that of the idler. Each point in the graph is calculated by two consecutive measurements of constructive and destructive interference, with the triangle/diamond markers representing the experimental data. As shown here, the visibility-transmission curve can be tailored to detect asymmetric loss, where the visibility can be up to twice as high when losses are applied on the signal than on the idler. Experimental error is up to $\pm 1.8\%$, as we show in the supplemental material.

was a Ti:Sapphire laser at 786nm (100mWatt average power, 8ps pulses), which was coupled into a photonic-crystal fiber (PCF) as the OPA to generate signal and idler pairs. We separated the signal, idler and pump beams in space using a prism pair, which also served as a phase control (using its variable dispersion). We applied optical loss independently on the signal and idler using two variable transmission filters. We then reflected the light back into the PCF for a second pass, where the nonlinear interference between signal-idler pairs and pump occurred.

The spectrum of the signal was then measured using a spectrometer, and the visibility was extracted from two consecutive measurements of constructive and destructive interference. We measured the visibility as a function of the transmissions of the signal (Fig. 3a) and the idler (Fig. 3b) separately for both the spontaneous ($n_i = 0$) and the strongly stimulated cases ($n_i = 10000$).

Apart from the variable loss filters, the experiment suffered internal loss due to the recoupling into the PCF and losses of optical elements. This inherent loss is not sym-

metric and resulted in different starting conditions in our system for the pump, signal and idler. We estimate the initial transmission of the signal and idler in this setup to be 52% and 42% respectively, while the parametric gains of the two amplifiers were $G_1 = 0.45, G_2 = 0.2$ (due to pump loss).

Our experimental results are shown in Fig. 3, where the inherent asymmetry in the losses can be observed from the visibility. In Fig. 3a, where the optical transmission of the signal is varied, the visibility increases in the stimulated case as the transmission of the signal decreases, reaching 92% at a signal transmission of 16%. This increase in visibility is attributed to loss-balancing of the signal and idler. The gain difference between OPA1 and OPA2 pushes the optimal visibility further towards lower signal transmission. On the other hand, increasing the loss of the idler, which had higher internal loss in the first place, always degrades the visibility (see Fig. 3b) for both the spontaneous and stimulated cases.

The vast difference in the visibility due to loss of the signal or of the idler can be exploited for sensing applications. For example, a medium with wavelength dependent absorption that is placed between the OPAs can be detected by observing its effect on the visibilities of the signal and the idler separately. The sensitivity of this detection can be optimized by asymmetric tuning of the losses and of the intensity of the seed. Specifically in the stimulated case of Fig. 3a, the slope of the visibility is large below 10% signal transmission, which is optimal for sensing the sample absorption at the signal wavelength in this SU(1,1) configuration. The same principles also enable to tailor the visibility-transmission curve for optimal detection of idler absorption, which would improve the quantum imaging performance of the interferometer [46–48].

Let us now consider how loss asymmetry affects the phase sensitivity of the SU(1,1) interferometer, which exploits the squeezing generated by the OPAs for sub shot-noise detection of phase. While high visibility is important for any phase-sensing experiment, it is not a direct indicator of sensitivity. Using error propagation analysis, the sensitivity of the interferometer (minimum detectable phase shift) is defined as

$$\Delta\theta^2 = \frac{\left\langle \hat{N}_s^2 \right\rangle - \left\langle \hat{N}_s \right\rangle^2}{\left| \frac{d}{d\theta} \right|_{\theta=\theta_0} \left\langle \hat{N}_s \right\rangle^2}, \quad (5)$$

where θ_0 is the phase-working point, around which small phase shifts $\Delta\theta$ are to be measured. Generally, the phase sensitivity of SU(1,1) depends the gain of each OPA, the internal photon loss and the phase-working point. For the ideal case (no loss, balanced amplifiers, coherently seeded idler) the sensitivity is:

$$\Delta\theta^2 = \frac{1}{(1+n_i) \sinh^2(2G)} = \frac{1}{4(1+n_i)(N_{sq}^2 + N_{sq})}, \quad (6)$$

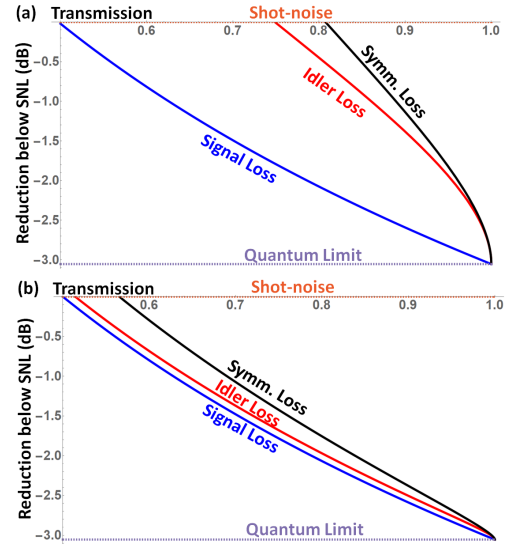


FIG. 4. The theoretical phase sensitivity (relative to the shot-noise) as a function of the transmission ($t_{s,i}^2$) of the signal (blue), idler (red) and equal transmission on both (black), for (a) the spontaneous $n_i = 0$ and (b) stimulated $n_i = 50$ cases, with $G_1 = G_2 = 0.1$. The dashed-orange curve at $y=0$ represents the classical shot-noise level (values below this level indicate squeezing), and the dashed-gray curve represents the limit of the ideal SU(1,1) interferometer. For the spontaneous case (a), loss on the measured mode (signal) achieves higher phase sensitivity than loss on the conjugated mode (idler). For the stimulated case (b) the gap between the curves closes, indicating that coherent stimulation on the conjugated mode increases its sensitivity in the presence of loss.

where $N_{sq} = \sinh^2(G)$ reflects the parametric gain in terms of the number of spontaneously generated photon-pairs. While the seeding term n_i has classical scaling, it is multiplied by the sub-shot-noise term of N_{sq}^2 . Since real-life sensing applications inherently require high photon flux, the coherent seed reinforces the low flux of squeezed photons with a high flux of coherent photons that stimulate the generation of pairs. While this stimulation does not increase the squeezing, it "upscales" the quantum effect to a higher range of optical intensities, greatly increasing its applicability.

We now discuss how stimulation can enhance the phase sensitivity in the presence of asymmetric internal loss. Following the error-propagation method of Eq. 5, we calculate the optimal phase sensitivity in the presence of loss: asymmetric (signal or idler) and symmetric (both). We normalize the phase-sensitivity relative to the shot-noise level, and explore both the spontaneous (Fig. 4a) and coherently seeded (Fig. 4b) regimes.

For the spontaneous SU(1,1) interferometer, a clear difference between the three cases is observed: signal-only loss (blue) shows the highest robustness to loss compared to idler-only (red) and symmetric (black) losses, which is the worst case. When a coherent seed is added, the signal-only case is unchanged (and remains optimal),

but the gap between the curves becomes smaller. This indicates that the stimulation can compensate for losses on the conjugated mode (idler).

Looking back at Fig. 2 and Fig. 4, we can see that the visibility and phase sensitivity seem to coincide in their response to asymmetric losses (blue and red lines), with signal loss being optimal, and idler loss closing the gap with the stimulation. In contrast, the case of symmetric (equal) loss has the highest visibility when stimulated, yet it achieves the worst sensitivity. This strengthens our previous statement that high visibility is not a direct indicator of optimal sensitivity and squeezing.

Our results are valuable for detection schemes that utilize one of the modes to sense the phase shift, with the other mode kept as loss-free as possible. In that regard, it is better to measure the mode that experiences the adverse losses instead of the conjugated mode. If the conjugated mode does experience loss, it can be compensated by seeding the interferometer. This can assist quantum illumination schemes [53–55], where one mode is used to sense a weakly reflecting target (experiencing major loss) with the other mode retained for reference. We also highlight the robustness of the $SU(1,1)$ interferometer, which was already shown to be effective against detection losses in past research [33, 56] and here expanded also to the case of asymmetric internal losses.

To conclude, we presented the analysis of asymmetric loss, measurement and seeding in the $SU(1,1)$ interferometer. We have shown that the visibility of interference can be used to distinguish between losses on the measured and conjugated modes, and that the visibility-transmission curve can be tailored by tuning the asymmetric parameters. We also analyzed the phase-sensitivity of the $SU(1,1)$ interferometer in the presence of asymmetric loss for the spontaneous and stimulated cases, where the coherent stimulation was able to mitigate for losses on the conjugated mode, therefore maintaining the sub-shot noise sensitivity. These results shed new light on the applicability of squeezing-based interferometers in the presence of asymmetric loss, and offer unexplored freedom for optimizing the detection with entangled pairs.

Acknowledgments. We thank Yuri Kaganovsky for producing the variable transmission filters and providing experimental insight. We thank our lab members for fruitful discussions.

E.C. and A.P. were supported by the Israel Innovation authority under grant 7002 and 73795. E.C. acknowledges support from the Quantum Science and Technology Program of the Israeli Council of Higher Education, from FQXi and from the Pazy foundation.

- [1] C. M. Caves, Quantum-mechanical noise in an interferometer, *Physical Review D* **23**, 1693 (1981).
- [2] Z. Y. Ou, Enhancement of the phase-measurement sensitivity beyond the standard quantum limit by a nonlinear interferometer, *Physical Review A* **85** (2012).
- [3] R. S. Bondurant and J. H. Shapiro, Squeezed states in phase-sensing interferometers, *Physical Review D* **30**, 2548 (1984).
- [4] C. M. Caves and B. L. Schumaker, New formalism for two-photon quantum optics. i. quadrature phases and squeezed states, *Physical Review A* **31**, 3068 (1985).
- [5] R. Schnabel, Squeezed states of light and their applications in laser interferometers, *Physics Reports* **684**, 1 (2017).
- [6] Y. Taguchi and Y. Ozeki, Time-domain analysis on the pulsed squeezed vacuum detected with picosecond pulses, *Journal of the Optical Society of America B* **37**, 1535 (2020).
- [7] R. F. Bishop and A. Vourdas, General two-mode squeezed states, *Z. Physik B - Condensed Matter* **71**, 527 (1988).
- [8] B. J. Lawrie, P. D. Lett, A. M. Marino, and R. C. Pooser, Quantum sensing with squeezed light, *ACS Photonics* **6**, 1307 (2019).
- [9] A. Schönbeck, F. Thies, and R. Schnabel, 13 dB squeezed vacuum states at 1550 nm from 12 mW external pump power at 775 nm, *Optics Letters* **43**, 110 (2017).
- [10] H. Grote, K. Danzmann, K. L. Dooley, R. Schnabel, J. Slutsky, and H. Vahlbruch, First long-term application of squeezed states of light in a gravitational-wave observatory, *Physical Review Letters* **110** (2013).
- [11] J. Aasi, J. Abadie, and B. P. A. et al., Enhanced sensitivity of the LIGO gravitational wave detector by using squeezed states of light, *Nature Photonics* **7**, 613 (2013).
- [12] L. McCuller, C. Whittle, D. Ganapathy, K. Komori, M. Tse, A. Fernandez-Galiana, L. Barsotti, P. Fritschel, M. MacInnis, F. Matichard, K. Mason, N. Mavalvala, R. Mittleman, H. Yu, M. Zucker, and M. Evans, Frequency-dependent squeezing for advanced LIGO, *Physical Review Letters* **124** (2020).
- [13] J. Miller, L. Barsotti, S. Vitale, P. Fritschel, M. Evans, and D. Sigg, Prospects for doubling the range of advanced LIGO, *Physical Review D* **91** (2015).
- [14] L. Barsotti, J. Harms, and R. Schnabel, Squeezed vacuum states of light for gravitational wave detectors, *Reports on Progress in Physics* **82**, 016905 (2018).
- [15] F. Acernese, Increasing the astrophysical reach of the advanced virgo detector via the application of squeezed vacuum states of light, *Physical Review Letters* **123** (2019).
- [16] F. Acernese, Quantum backaction on kg-scale mirrors: Observation of radiation pressure noise in the advanced virgo detector, *Physical Review Letters* **125** (2020).
- [17] L. Pezzé and A. Smerzi, Mach-zehnder interferometry at the heisenberg limit with coherent and squeezed-vacuum light, *Physical Review Letters* **100** (2008).
- [18] K. Wodkiewicz and J. H. Eberly, Coherent states, squeezed fluctuations, and the $SU(2)$ am $SU(1,1)$ groups in quantum-optics applications, *Journal of the Optical Society of America B* **2**, 458 (1985).
- [19] G. Cerullo and S. D. Silvestri, Ultrafast optical parametric amplifiers, *Review of Scientific Instruments* **74**, 1

(2003).

[20] L. Bello, Y. Michael, M. Rosenbluh, E. Cohen, and A. Pe'er, Complex two-mode quadratures – a unified formalism for continuous-variable quantum optics, arXiv (2020), 2011.08099v1.

[21] B. L. Schumaker and C. M. Caves, New formalism for two-photon quantum optics. II. mathematical foundation and compact notation, *Physical Review A* **31**, 3093 (1985).

[22] C. M. Caves, Reframing $SU(1,1)$ interferometry, *Advanced Quantum Technologies* **3**, 1900138 (2020).

[23] L.-L. Guo, Y.-F. Yu, and Z.-M. Zhang, Improving the phase sensitivity of an $SU(1,1)$ interferometer with photon-added squeezed vacuum light, *Optics Express* **26**, 29099 (2018).

[24] B. Yurke, S. L. McCall, and J. R. Klauder, $SU(2)$ and $SU(1,1)$ interferometers, *Physical Review A* **33**, 4033 (1986).

[25] M. V. Chekhova and Z. Y. Ou, Nonlinear interferometers in quantum optics, *Advances in Optics and Photonics* **8**, 104 (2016).

[26] Z. Y. Ou and X. Li, Quantum $SU(1,1)$ interferometers: Basic principles and applications, *APL Photonics* **5**, 080902 (2020).

[27] B. E. Anderson, B. L. Schmittberger, P. Gupta, K. M. Jones, and P. D. Lett, Optimal phase measurements with bright- and vacuum-seeded $SU(1,1)$ interferometers, *Physical Review A* **95** (2017).

[28] D. Li, B. T. Gard, Y. Gao, C.-H. Yuan, W. Zhang, H. Lee, and J. P. Dowling, Phase sensitivity at the heisenberg limit in an $SU(1,1)$ interferometer via parity detection, *Physical Review A* **94** (2016).

[29] P. Gupta, B. L. Schmittberger, B. E. Anderson, K. M. Jones, and P. D. Lett, Optimized phase sensing in a truncated $SU(1,1)$ interferometer, *Optics Express* **26**, 391 (2018).

[30] N. Prajapati and I. Novikova, Polarization-based truncated $SU(1,1)$ interferometer based on four-wave mixing in rb vapor, *Optics Letters* **44**, 5921 (2019).

[31] Y. Shaked, Y. Michael, R. Z. Vered, L. Bello, M. Rosenbluh, and A. Pe'er, Lifting the bandwidth limit of optical homodyne measurement with broadband parametric amplification, *Nature Communications* **9** (2018).

[32] J. Li, Y. Liu, N. Huo, L. Cui, C. Feng, Z. Y. Ou, and X. Li, Pulsed entanglement measured by parametric amplifier assisted homodyne detection, *Optics Express* **27**, 30552 (2019).

[33] M. Manceau, G. Leuchs, F. Khalili, and M. Chekhova, Detection loss tolerant supersensitive phase measurement with an $SU(1,1)$ interferometer, *Physical Review Letters* **119** (2017).

[34] M. Manceau, F. Khalili, and M. Chekhova, Improving the phase super-sensitivity of squeezing-assisted interferometers by squeeze factor unbalancing, *New Journal of Physics* **19**, 013014 (2017).

[35] T. Li, B. E. Anderson, T. Horrom, B. L. Schmittberger, K. M. Jones, and P. D. Lett, Improved measurement of two-mode quantum correlations using a phase-sensitive amplifier, *Optics Express* **25**, 21301 (2017).

[36] Y. Michael, L. Bello, M. Rosenbluh, and A. Pe'er, Squeezing-enhanced Raman spectroscopy, *npj Quantum Information* **5** (2019).

[37] N. Prajapati, Z. Niu, and I. Novikova, Quantum-enhanced two-photon spectroscopy using two-mode squeezed light, *Optics Letters* **46**, 1800 (2021).

[38] R. Pooser, N. Savino, E. Batson, J. Beckey, J. Garcia, and B. Lawrie, Truncated nonlinear interferometry for quantum-enhanced atomic force microscopy, *Physical Review Letters* **124**, 230504 (2020).

[39] R. Z. Vered, Y. Shaked, Y. Ben-Or, M. Rosenbluh, and A. Pe'er, Classical-to-quantum transition with broadband four-wave mixing, *Physical Review Letters* **114** (2015).

[40] W. N. Plick, J. P. Dowling, and G. S. Agarwal, Coherent-light-boosted, sub-shot noise, quantum interferometry, *New Journal of Physics* **12**, 083014 (2010).

[41] D. Li, C.-H. Yuan, Z. Y. Ou, and W. Zhang, The phase sensitivity of an $SU(1,1)$ interferometer with coherent and squeezed-vacuum light, *New Journal of Physics* **16**, 073020 (2014).

[42] A. M. Marino, N. V. C. Trejo, and P. D. Lett, Effect of losses on the performance of an $SU(1,1)$ interferometer, *Physical Review A* **86** (2012).

[43] X.-L. Hu, D. Li, L. Q. Chen, K. Zhang, W. Zhang, and C.-H. Yuan, Phase estimation for an $SU(1,1)$ interferometer in the presence of phase diffusion and photon losses, *Physical Review A* **98** (2018).

[44] J. Xin, H. Wang, and J. Jing, The effect of losses on the quantum-noise cancellation in the $SU(1,1)$ interferometer, *Applied Physics Letters* **109**, 051107 (2016).

[45] G. B. Lemos, V. Borish, G. D. Cole, S. Ramelow, R. Lapkiewicz, and A. Zeilinger, Quantum imaging with undetected photons, *Nature* **512**, 409 (2014).

[46] D. A. Kalashnikov, A. V. Paterova, S. P. Kulik, and L. A. Krivitsky, Infrared spectroscopy with visible light, *Nature Photonics* **10**, 98 (2016).

[47] A. V. Paterova, S. M. Maniam, H. Yang, G. Grenci, and L. A. Krivitsky, Hyperspectral infrared microscopy with visible light, *Science Advances* **6**, eabd0460 (2020).

[48] I. Kviatkovsky, H. M. Chrzanowski, E. G. Avery, H. Bartolomaeus, and S. Ramelow, Microscopy with undetected photons in the mid-infrared, *Science Advances* **6** (2020).

[49] J.-P. W. MacLean, J. M. Donohue, and K. J. Resch, Direct characterization of ultrafast energy-time entangled photon pairs, *Physical Review Letters* **120** (2018).

[50] Z. Yang, P. Saurabh, F. Schlawin, S. Mukamel, and K. E. Dorfman, Multidimensional four-wave-mixing spectroscopy with squeezed light, *Applied Physics Letters* **116**, 244001 (2020).

[51] A. Pe'er, B. Dayan, A. A. Friesem, and Y. Silberberg, Temporal shaping of entangled photons, *Physical Review Letters* **94** (2005).

[52] A. L. Porta and R. E. Slusher, Squeezing limits at high parametric gains, *Physical Review A* **44**, 2013 (1991).

[53] S.-H. Tan, B. I. Erkmen, V. Giovannetti, S. Guha, S. Lloyd, L. Maccone, S. Pirandola, and J. H. Shapiro, Quantum illumination with gaussian states, *Physical Review Letters* **101** (2008).

[54] J. H. Shapiro, The quantum illumination story, *IEEE Aerospace and Electronic Systems Magazine* **35**, 8 (2020).

[55] R. Nair and M. Gu, Fundamental limits of quantum illumination, *Optica* **7**, 771 (2020).

[56] G. Frascella, S. Agne, F. Y. Khalili, and M. V. Chekhova, Overcoming detection loss and noise in squeezing-based optical sensing, *npj Quantum Information* **7** (2021).